

Thermal Evolution and Instability of CO-Induced Platinum Clusters on the Pt(557) Surface at Ambient Pressure

Jeongjin Kim,^{†,‡} Myung Cheol Noh,^{†,‡} Won Hui Doh,^{†,‡} and Jeong Young Park^{*,†,‡}

[†]Center for Nanomaterials and Chemical Reactions, Institute for Basic Science, Daejeon 34141, Republic of Korea

[‡]Graduate School of EEWS, Korea Advanced Institute of Science and Technology, Daejeon 34141, Republic of Korea

S Supporting Information

ABSTRACT: Carbon monoxide (CO) is one of the most-studied molecules among the many modern industrial chemical reactions available. Following the Langmuir–Hinshelwood mechanism, CO conversion starts with adsorption on a catalyst surface, which is a crucially important stage in the kinetics of the catalytic reaction. Stepped surfaces show enhanced catalytic activity because they, by nature, have dense active sites. Recently, it was found that surface-sensitive adsorption of CO is strongly related to surface restructuring via roughening of a stepped surface. In this scanning tunneling microscopy study, we observed the thermal evolution of surface restructuring on a representative stepped platinum catalyst, Pt(557). CO adsorption at 1.4 mbar CO causes the formation of a broken-step morphology, as well as CO-induced triangular Pt clusters that exhibit a reversible disordered–ordered transition. Thermal instability of the CO-induced platinum clusters on the stepped surface was observed, which is associated with the reorganization of the repulsive CO–CO interactions at elevated temperature.

Industrial chemical reactions related to CO conversion (e.g., CO oxidation, Fischer–Tropsch, and water–gas–shift) commonly occur on the catalyst surface, which starts with chemisorption of a CO molecule according to the Langmuir–Hinshelwood mechanism. Typically, the reaction rates of these industrial chemical reactions are tailored by an optimized ratio of reactant molecules. To achieve highly enhanced catalytic activity, an understanding of each chemical reaction step on a specific facet of the catalyst surface is required in order to design thermodynamically rational reaction pathways. Especially, CO adsorption is the dominating reaction step because of the limited number of adsorption and active sites on a specifically defined surface area, which could restrict catalytic activity. There have been many significant studies investigating the fundamental chemisorbed CO surface structures on platinum (Pt) as a function of CO coverage; model systems have been analyzed using low-energy electron diffraction (LEED) patterns, temperature-programmed desorption (TPD), infrared reflection–absorption spectroscopy (IRAS), and electron energy loss spectroscopy (EELS) on flat and stepped Pt surfaces.^{1–3} These studies show that when CO molecules are adsorbed on the flat Pt(111) surface, they show a $(\sqrt{3} \times \sqrt{3})R30^\circ$ structure at $\theta = 0.33$, a $c(4 \times 2)$ structure at $\theta = 0.5$, and a reversible ordered–

disordered phenomenon above $\theta = 0.5$, which implies short-range CO–CO repulsive interactions affect CO adsorption.^{1,4} However, these modern surface science techniques were carried out in ultrahigh vacuum (UHV) at low temperature because of innate heterogeneous interface limitations found in the UHV-based techniques that are related to the length of the electron mean free path.^{5,6} These conditions are definitely far from the “real world” conditions found in industrial chemical reactors.⁷ The pressure gap between UHV and atmosphere at room temperature (RT) creates a difference of ~ 0.3 eV of surface free energy, as calculated using fundamental thermodynamics, which is enough to change both surface structure and stability.^{8,9}

Interestingly, step sites on a surface have a relatively higher coverage of adsorbed CO compared with a flat terrace;^{2,10} the stepped Pt(557) surface could have an almost fully saturated surface coverage ($\theta = 1$) of adsorbed CO molecules at high pressure by virtue of its dense, narrow steps.¹¹ This inherent structural peculiarity implies that many metastable adsorbate-mediated Pt atoms restructure vertically on the surface. This phenomenon takes place until the Pt atoms reach chemical equilibrium.¹²

To better represent industrial catalytic conditions, we used ambient-pressure scanning tunneling microscopy (AP-STM) to monitor the CO-induced restructured Pt(557) surface at 1.4 mbar of CO and at elevated temperatures. We obtained STM images at 1.4 mbar of CO and at RT that consist of randomly oriented triangular Pt clusters that result from the strong CO–CO repulsive interactions on the stepped Pt(557) surface.¹³ However, we observed partially ordered periodic triangular Pt clusters on the Pt(557) surface at elevated temperatures up to 373 K. In addition, reversible disordered–ordered transitions were also observed in cycles of *operando* experimental conditions. These unexpected results imply that there is an intrinsic relation between the density of the CO adsorbate and the number of defect sites on a stepped surface at elevated temperature.

All of the experimental procedures were performed using an AP-STM instrument with an integrated reaction cell (SPECS GmbH). The Pt(557) single crystal (MaTeck GmbH) was cleaned by repeated cycles of Ar⁺ sputtering, O₂ annealing, and flash-annealing in UHV to obtain a well-prepared atomic step-terrace Pt(557) surface. The atomically resolved clean Pt(557) surface image (Figure S1 in the Supporting Information) exhibits a periodic structure with a Pt–Pt nearest-neighbor spacing

Received: October 18, 2015

Published: January 19, 2016

distance of ~ 0.280 nm, which is similar to that commonly known from the literature for Pt(111) (i.e., 0.277 nm).

Figure 1 shows representative STM images obtained on the Pt(557) surface with schematic models of the surface at the

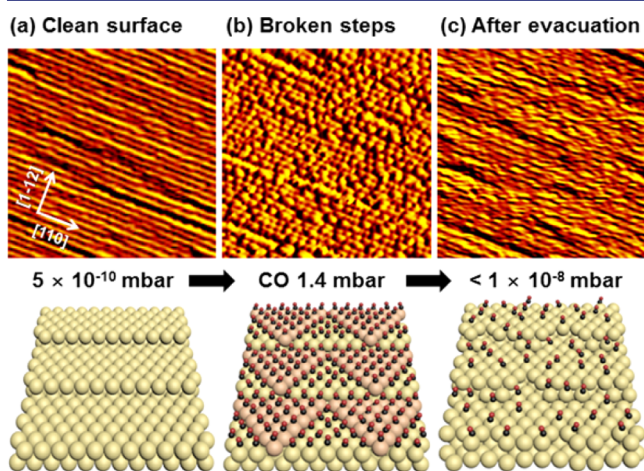


Figure 1. (Top) STM images ($40 \text{ nm} \times 40 \text{ nm}$) of Pt(557) at the different gas conditions. (Bottom) Schematic diagrams of the respective STM images. STM images of (a) an atomically clean surface obtained at 5×10^{-10} mbar, (b) randomly formed step-break CO-induced Pt clusters obtained at 1.4 mbar CO, and (c) the surface after evacuation.

different pressures of the reaction cell. The clean Pt(557) surface (Figure 1a) has a 1.3 nm step width along the $[1-12]$ direction and a 2.2 Å step height. These measurements are very well matched with theoretical models and previous studies.^{13,14} When CO molecules were introduced over the Pt(557) in a reaction cell at 1.4 mbar of CO, the step height on the Pt cluster surface nearly doubled (Figure 1b). After evacuation, the restructured Pt clusters disappeared, as shown in Figure 1c. The lifted $[001]$ direction of the step height still remained after evacuation with a pressure of $< 1 \times 10^{-8}$ mbar. The ordinary, clean Pt(557) surface changed dramatically with the introduction of CO molecules at ambient pressure. The CO molecules adsorbed on each Pt atom at a ratio of almost 1:1 with strong CO–CO repulsive interactions. These results suggest that adsorbate-induced restructuring at high CO coverage is greatly influenced by the presence of defect sites (e.g., steps, kinks, and vacancies). This finding is markedly different from the traditional surface analysis results at UHV; there are no free molecules at UHV that are able to be weakly bound to the metal surface because they have chemical potentials equivalent to the pressure gap. Surface CO coverages of 1 and 0.5, corresponding to Figure 1b and 1c, respectively, were determined from ambient-pressure X-ray photoelectron spectroscopy (AP-XPS) results.¹³ The number of low-coordinated Pt atoms increases because the metal-bound CO molecules tilt to relax the CO–CO repulsive interactions. Pt atoms are lifted vertically because the CO-bound step-edge Pt atoms burrow downward; this mechanism for the creation of the Pt clusters is supported by theoretical calculation results.^{12,13} As mentioned above, the strong CO–CO repulsive interactions occurred at very close range (~ 5 Å); thus, the CO molecules were bent to avoid each other.^{15,16} This tilting angle is probably influenced by the relaxed geometry of the low coordinated number of the Pt surface atom sites.¹⁷ To study the temperature dependence of the repulsive interaction among the CO molecules, we gradually raised the temperature.

Figure 2 shows disordered Pt clusters at 1.4 mbar of CO and RT and ordered Pt cluster rearrangements caused by the raised

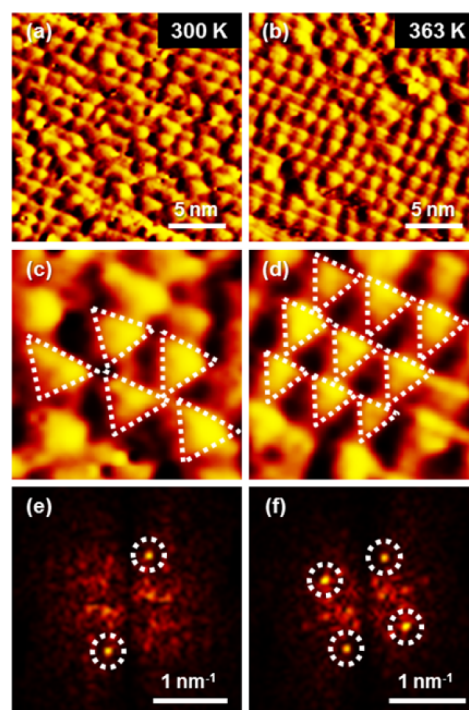


Figure 2. Comparison of STM images for disordered–ordered CO-induced restructuring for Pt cluster formation on the Pt(557) surface at (a) 300 and (b) 363 K; (c, d) $6 \text{ nm} \times 6 \text{ nm}$ enlarged images from (a) and (b), respectively; and (e, f) fast Fourier transformation (FFT) results from (a) and (b), respectively.

temperature (i.e., 363 K). We observed this trend in the STM images (Figure 2a,b) taken at 300 and 363 K, respectively. Figure 2c (taken at 300 K) and 2d (363 K) are magnified images from Figure 2a and 2b, respectively, which display a clear trend of Pt cluster rearrangement. The roughly formed triangular shape of the Pt clusters are ~ 2 nm in size, which shows a periodicity identified by fast Fourier transformation (FFT) at 300 K (Figure 2e). Interestingly, the partially ordered Pt clusters at 363 K have another periodicity that was confirmed by FFT analysis (Figure 2f): the cluster size shrank to ~ 1.5 nm along both directions (i.e., $[110]$ and $[1-12]$ on the Pt(557) surface).

Previous high-pressure sum-frequency generation (SFG) results revealed that spectroscopic mode change behavior is caused by adsorbed molecules on the top sites of the Pt(557) surface at elevated temperature. The CO stretch vibrational mode is shifted to a frustrated translational mode¹⁸ on the Pt(557) surface before CO dissociation occurred on the step sites as the temperature increased to over 548 K.^{11,19} The CO molecules would be adsorbed either on step or terrace sites, depending on the CO coverage. It was also shown that desorption occurs on terrace sites at 450 K and on step sites at 540 K.¹⁰ Moreover, molecules that desorb incompletely are dissociated via the exothermic Boudouard reaction ($2\text{CO} \rightarrow \text{C} + \text{CO}_2$) on the Pt(557) surface.²⁰ We deliberately performed our STM observations at temperatures below 380 K and at a pressure of 1.4 mbar of CO to avoid the influence of extensive amounts of weakly bound CO molecules desorbing. Several STM observations at ambient pressures of CO showed CO-adsorbed incommensurate ($\sqrt{19} \times \sqrt{19}$)R23.4° superstructures as well

as moiré patterns on Pt(111) at pressures above 700 Torr^{21,22} and free CO molecules exposing a broken-up stepped surface on Pt(557) at 0.1 Torr,¹³ which provide additional insight to the *in situ* gas/solid interface. These results reveal that the formation of a CO-induced restructured surface or Pt clusters can be clearly attributed to the pressure gap. Nonetheless, the observations were not conducted at temperatures high enough to activate the chemical reactions, but at RT. The adsorbed molecules diffused to find another reactant to stabilize their own thermodynamic energy via chemical reaction and desorption from the surface;²³ however, the elevated temperature leads to a more thermodynamically unstable situation that is needed to push the chemical reaction forward. Consequently, the Pt cluster rearrangement phenomenon would occur in a region with similar thermally evolved vibrational mode changes. Additionally, the migration of adsorbed CO molecules from a step to a terrace site is not likely.^{18,24} However, adjacent Pt atom extractions from the surface lattice (i.e., that are influenced by Pt carbonyl species) are still possible as the temperature increases. This is a driving force for Pt atoms to migrate to fresh defect sites;²⁵ thus, the species could nucleate clusters to reconstruct or transform the metal surface.^{26,27} The structure sensitivity of the CO-induced restructured surface is correlated with the CO chemisorption energy on a specific site and the *d*-band shift of the Pt atoms' electronic structure; the energy variation is not negligible (i.e., as much as 1 eV).²⁸ Therefore, there is an energetically probable competition between CO-induced restructuring of defect sites and spontaneous cluster nucleation on the thermally evolved stepped Pt(557) surface.

We observed a dynamic cluster rearrangement to form partially ordered structures, as shown in Figure 3. The figure

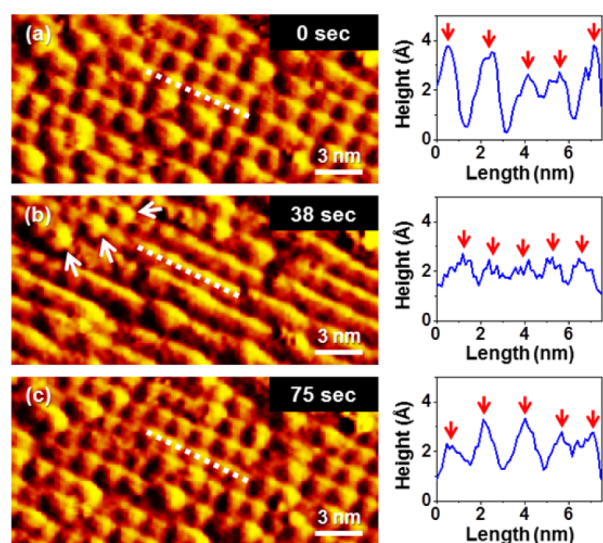


Figure 3. (Left) *Operando* STM images of CO-induced Pt cluster restructuring on the Pt(557) surface at 347 K, and (right) representative line profiles of the clusters. Each image illustrates the clusters found after 0, 38, and 75 s (a, b, and c, respectively). CO pressure is 1.4 mbar.

shows a series of STM images of the Pt(557) surface and representative cluster height line profiles with time. The triangular Pt clusters were initially ~ 4 Å in height (Figure 3a). After 38 s, they shrunk and became similar to an almost flat terrace (Figure 3b). Finally, corrugation from clusters was revealed again (Figure 3c), but the clusters had rearranged their positions and showed compressed cluster heights. We note that

the clusters marked by arrows in Figure 3b appear to be the same in Figure 3a–c, indicating that thermal evolution of the Pt clusters takes place in a localized region. From the similarities between the three images, we can also rule out the issue of tip artifacts caused by the adsorption of a hydrocarbon on the STM tip, which would change the entire image following the adsorption event. The statistical histogram analysis results show that the Pt clusters' corrugation height distribution changed with time (Figure S2).

It seems that the thermally evolved unstable Pt clusters are rearranged until they reach equilibrium. When the temperature was above 350 K, we observed both neat and noisy STM images caused by massive diffusion of CO or step-edge atoms while the surface stabilized to equilibrium. Former *operando* AP-STM studies clearly demonstrated dynamic surface evolution that moved toward thermodynamic equilibrium or intermediate transitions on Pt(111),²⁹ Pt(110),³⁰ Cu(110),³¹ and Co(0001).³² Unfortunately, the time resolution of the STM technique ($\sim 10^0$ – 10^2 s/image) is not sufficient to investigate surface changes caused by the fine vibrational resonance of the adsorbates or atomic-scale diffusion at RT ($\sim 10^{-12}$ – 10^{-6} s/atom) due to the extreme differences in time scale. Therefore, in principle, it is impossible to visualize the dynamic atomic-scale surface evolution. We suppose that each STM image shows a thermodynamically stable surface at an intermediate stage during the rearrangement of the Pt clusters at a given moment.

The relation between temperature and the distribution of the deviation of Pt cluster corrugation heights is indicated by representative STM images of the disordered–ordered transitions in Figure 4. Statistical histogram analysis of the Pt cluster

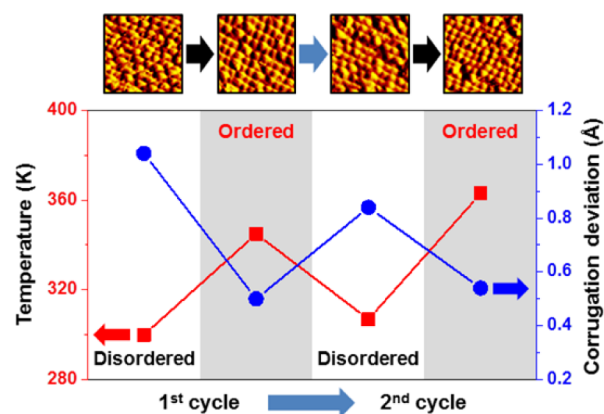


Figure 4. Plot of Pt cluster heights and temperatures during two heating–cooling cycles on the Pt(557) surface. STM images (15 nm \times 15 nm) show that the disordered–ordered transition is reversible.

corrugation height is shown in Figure S3. The temperature–height–distribution relation appears to be consistent in spite of performing two heating–cooling cycles. This suggests that the appearance of a partially ordered structure on the Pt(557) surface is not a coincidence. The average Pt cluster corrugation height at elevated temperatures was reduced by roughly 10% from the initial disordered structure. The above-mentioned direct observations indicate the reversible formation of ordered Pt cluster structures on Pt(557) at temperatures over 345 K. We suppose that this reversible phenomenon takes place because of the competing processes of surface roughening and adsorbate dissociation. The CO-induced restructured Pt(557) surface would atomically rearrange through two competitive driving

forces as follows: First, the randomly piled triangular Pt clusters degraded to Pt atoms and introduced more defect sites by thermal evolution. Second, the restructured Pt atoms nucleated immediately on account of the reorganized CO–CO repulsive interactions at low-coordinated step sites. In this process, the most optimized size and shape of the Pt clusters is possibly observed (i.e., instead of randomly distributed larger sizes of Pt clusters) at elevated temperatures before the adsorbed CO molecules dissociate on the Pt(557) surface.

In summary, the instability of triangular Pt clusters on the Pt(557) surface at 1.4 mbar of CO was observed by *operando* AP-STM at elevated temperatures. We observed disordered–ordered transitions of CO-induced triangular Pt clusters at 363 K. Thermal evolution broke the surface geometric equilibrium of a randomly disordered Pt cluster structure with the introduction of more defect sites on the Pt(557) surface. The Pt atoms were then simultaneously rearranged at low-coordinated step sites by CO–CO repulsive interactions to form partially ordered triangular Pt clusters. Furthermore, surface fluctuations between the triangular and almost flat shapes were observed along the [110] direction on the wide Pt(557) terrace. Statistical analysis of the Pt cluster height shows that the vertical corrugation of the ordered surface has a much narrower distribution (i.e., about half that of the disordered surface).

■ ASSOCIATED CONTENT

📄 Supporting Information

The Supporting Information is available free of charge on the ACS Publications website at DOI: 10.1021/jacs.5b10628.

Experimental details and Figures S1–S3 (PDF)

■ AUTHOR INFORMATION

Corresponding Author

*jeongypark@kaist.ac.kr

Notes

The authors declare no competing financial interest.

■ ACKNOWLEDGMENTS

This work was supported by IBS-R004-G4.

■ REFERENCES

- (1) Ertl, G.; Neumann, M.; Streit, K. M. *Surf. Sci.* **1977**, *64*, 393.
- (2) Hopster, H.; Ibach, H. *Surf. Sci.* **1978**, *77*, 109.
- (3) Persson, B. N. J.; Tüshaus, M.; Bradshaw, A. M. *J. Chem. Phys.* **1990**, *92*, 5034.
- (4) Heyden, B. E.; Bradshaw, A. M. *Surf. Sci.* **1983**, *125*, 787.
- (5) Somorjai, G. A.; Park, J. Y. *Phys. Today* **2007**, *60*, 48.
- (6) Somorjai, G. A.; Park, J. Y. *J. Chem. Phys.* **2008**, *128*, 182504.
- (7) Somorjai, G. A.; Park, J. Y. *Surf. Sci.* **2009**, *603*, 1293.
- (8) Somorjai, G. A.; York, R. L.; Butcher, D.; Park, J. Y. *Phys. Chem. Chem. Phys.* **2007**, *9*, 3500.
- (9) Salmeron, M.; Schlögl, R. *Surf. Sci. Rep.* **2008**, *63*, 169.
- (10) Ohno, Y.; Sanchez, J. R.; Lesar, A.; Yamanaka, T.; Matsushima, T. *Surf. Sci.* **1997**, *382*, 221.
- (11) McCrea, K.; Parker, J. S.; Chen, P.; Somorjai, G. *Surf. Sci.* **2001**, *494*, 238.
- (12) Michalka, J. R.; McIntyre, P. W.; Gezelter, J. D. *J. Phys. Chem. C* **2013**, *117*, 14579.
- (13) Tao, F.; Dag, S.; Wang, L.-W.; Liu, Z.; Butcher, D. R.; Bluhm, H.; Salmeron, M.; Somorjai, G. A. *Science* **2010**, *327*, 850.
- (14) Zhu, Z.; Tao, F.; Zheng, F.; Chang, R.; Li, Y.; Heinke, L.; Liu, Z.; Salmeron, M.; Somorjai, G. A. *Nano Lett.* **2012**, *12*, 1491.
- (15) Weymouth, A. J.; Hofmann, T.; Giessibl, F. J. *Science* **2014**, *343*, 1120.

- (16) Salmeron, M. *Science* **2014**, *343*, 1083.
- (17) Frenken, J. W. M.; Stoltze, P. *Phys. Rev. Lett.* **1999**, *82*, 3500.
- (18) Jänsch, H. J.; Xu, J.; Yates, J. T. *J. Chem. Phys.* **1993**, *99*, 721.
- (19) McCrea, K. R.; Parker, J. S.; Somorjai, G. A. *J. Phys. Chem. B* **2002**, *106*, 10854.
- (20) Kung, K. Y.; Chen, P.; Wei, F.; Shen, Y. R.; Somorjai, G. A. *Surf. Sci.* **2000**, *463*, L627.
- (21) Jensen, J. A.; Rider, K. B.; Salmeron, M.; Somorjai, G. A. *Phys. Rev. Lett.* **1998**, *80*, 1228.
- (22) Longwitz, S. R.; Schnadt, J.; Vestergaard, E. K.; Vang, R. T.; Stensgaard, L.; Brune, H.; Besenbacher, F. *J. Phys. Chem. B* **2004**, *108*, 14497.
- (23) Jiang, P.; Bao, X.; Salmeron, M. *Acc. Chem. Res.* **2015**, *48*, 1524.
- (24) Xu, J.; Yates, J. T. *J. Chem. Phys.* **1993**, *99*, 725.
- (25) Somorjai, G. A.; Contreras, A. M.; Montano, M.; Rioux, R. M. *Proc. Natl. Acad. Sci. U. S. A.* **2006**, *103*, 10577.
- (26) Ritter, E.; Behm, R. J.; Pötschke, G.; Wintterlin, J. *Surf. Sci.* **1987**, *181*, 403.
- (27) Gritsch, T.; Coulman, D.; Behm, R. J.; Ertl, G. *Phys. Rev. Lett.* **1989**, *63*, 1086.
- (28) Hammer, B.; Nielsen, O. H.; Nørskov, J. K. *Catal. Lett.* **1997**, *46*, 31.
- (29) Nguyen, L.; Cheng, F.; Zhang, S.; Tao, F. *J. Phys. Chem. C* **2013**, *117*, 971.
- (30) Hendriksen, B. L. M.; Frenken, J. W. M. *Phys. Rev. Lett.* **2002**, *89*, 046101.
- (31) Xu, F.; Mudiyanse, K.; Baber, A. E.; Soldemo, M.; Weissenrieder, J.; White, M. G.; Stacchiola, D. J. *J. Phys. Chem. C* **2014**, *118*, 15902.
- (32) Ehrensperger, M.; Wintterlin, J. *J. Catal.* **2015**, *329*, 49.